EPJ Web of Conferences **17**, 16018 (2011)
DOI: 10.1051/epjconf/20111716018

Fusion, elastic and total reaction cross sections in the collision $^{6}Li+^{64}Zn$

D. Torresi[1,2,a], A. Di Pietro[1], E. Strano[1,2], M. Zadro[4], P. Figuera[1], M. Fisichella[1,3], M. Lattuada[1,2], C. Maiolino[1], A. Musumarra[1], M.G. Pellegriti[1], D. Santonocito[1,2], and V. Scuderi[1,]

[1] INFN Laboratori Nazionali del Sud, Catania, Italy
[2] Dipartimento di Fisica ed Astronomia, Università di Catania, Catania, Italy
[3] Università degli studi di Messina, Messina, Italy
[4] Rudjer Boskovic Institute, Zagreb, Croatia

Abstract. The structure of the weakly bound nuclei is expected to influence the fusion mechanism at energies around and below the Coulomb barrier. Infact direct channels may be favoured with respect to fusion by the low binding energies, while Coupling of the break-up channel can be responsible for a fusion cross-section enhancement. In this context the $^{6}Li+^{64}Zn$ collision has been studied at several energies around the Coulomb barrier. The fusion cross section was measured by using an activation technique where the radioactive evaporation residues produced in the reaction were identified by the X-ray emission which follows their electron capture decay. The elastic scattering angular distributions were analyzed within the Optical Model and total reaction cross-sections were deduced from optical model calculations.

1 Introduction

Weakly bound nuclei are nuclear systems with the ground state energy very close to the particle emission threshold. Thus a small ammount of energy is enough to break-up the nucleus into two or more parts. In collisions involving a weakly bound nucleus direct processes like break-up and transfer may be favoured by the low binding energy and/or cluster structure [1]. From a static point of view, a diffused mass distribution affects the projectile-target potential lowering the Coulomb barrier and increasing the fusion cross section; from a dynamical point of view, it is known that the strong coupling of the entrance channel with inelastic excitation or other reaction channels like break-up may lead to an enhancement of the fusion cross section with respect to single barrier penetration model. On the other hand the break-up channel removes flux from fusion suppressing it.

In order to investigate the previously discussed topic, the goal of the present experiment is to study the collisions induced by ^{6}Li and ^{7}Li on a ^{64}Zn target.

^{6}Li and ^{7}Li are both weakly bound nuclei but there are differences in their structure: ^{6}Li does not have bounded excited states and its binding energy is 1.4 MeV; ^{7}Li has a bound excited state at 0.5 MeV and its binding energy is 2.5 MeV. Possible effects of these differences on reaction dynamics are discussed in [2], where are investigated the collisions induced by ^{6}Li and ^{7}Li on a ^{59}Co target. At sub-barrier energies, it has been observed a ^{6}Li total fusion cross-section enhancement with respect to the ^{7}Li total fusion cross-section. The authors concluded that this behaviour could be explained only taking into account the coupling with the break-up and the different binding energy of the two nuclei. For this reason we want to measure the $^{6,7}Li+^{64}Zn$ total fusion excitation functions down to energies far below the Coulomb barrier. Although the complete goal of the present experiment is a comparison of the results for the systems $^{6,7}Li+^{64}Zn$, here only results from the $^{6}Li+^{64}Zn$ system will be discussed.

[a] e-mail: torresir@lns.infn.it

2 Total fusion cross section.

2.1 Experimental technique.

The $^{6}Li+^{64}Zn$ experiment was performed at Laboratori Nazionali del Sud in Catania (Italy). The ^{6}Li beam was provided at E_{lab} ranging from 11 to 22 MeV. The fusion excitation function was performed using the activation technique [9,4]. The direct detection of evaporated residues (ER), produced in the collision of a low energy light projectile onto a medium mass target is not always possible since the largest fraction of ER will not come out from the target owing to the their low kinetic energy. However it is possible to choose a target in such a way that almost all the evaporation residues decay by electron capture (EC). Detecting the atomic X-ray emitted after the EC decay it is possible to estimate the ammount of evaporation residues produced during the activation and then the total fusion cross-section.

The activation technique, used in the present experiment, consists of two steps. In the first step the target is activated. During this time the Zn target (250-550 g/cm^{2}) is first irradiated with the ^{6}Li beam monitoring the beam current. The fusion-evaporation reactions take place within the target and the largest fraction of ER produced will not come

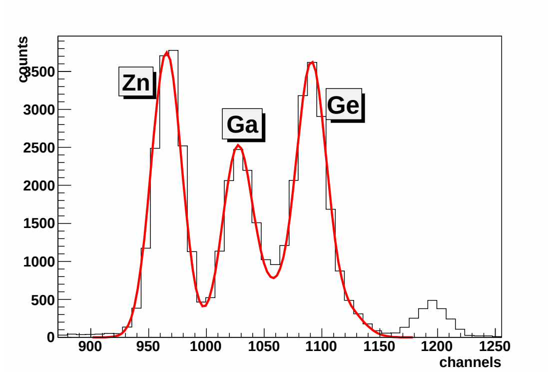

Fig. 1. Typical X-ray spectrum measured off-line for the reaction ^{6}Li+^{64}Zn. It is possible to distinguish three main peaks which correspond to the K_α X-ray emission lines of Zn, Ga and Ge.

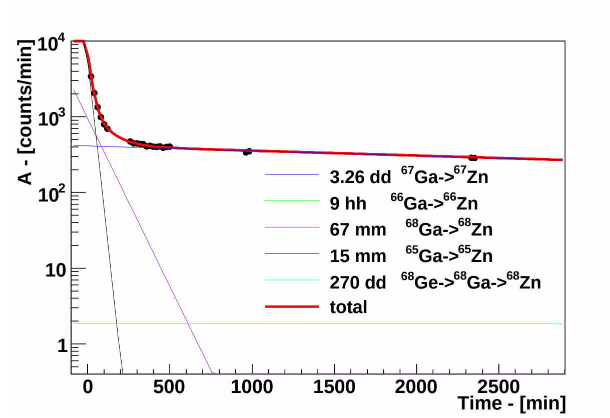

Fig. 2. Activity curve for the Ga isotopes.

out from it. The small fraction of residues emerging from the target is stopped in the catcher (^{93}Nb or ^{197}Au) placed behind the target. At the end of the irradiation time the activated target and catcher are placed very close to the Si(Li) detector to measure the residues activity. One of the advantages of this technique is the 100% intrinsic detection efficiency of Si(Li) detector in the energy region of interest (7-11 KeV). Moreover the atomic X-ray in this energy region can be detected with extremely low background.

2.2 Experimental results.

In figure 1 typical X-ray spectra measured off-line for the reaction ^{6}Li+^{64}Zn are shown. The fit of the spectrum was performed by using five gaussian functions that take into account the K_α X-ray emission lines for Zn, Ga and Ge and K_β for Zn and Ga. The present analysis was performed taking into account only the K_α emission lines. From the X-ray energies it is possible to identify different elements. In order to discriminte different isotopes it is required following the X-ray activity as a function of time. For each element the activity curve is obtained by fitting the measured activity experimental points by using a sum of several exponential functions with different decay time, one for each isotopes. As example, in figure 2 is shown the activity curve of Ga isotopes. It is a sum of four different esponential functions which decay time range from few minutes to several days. The activity at the end of the activation (origin of the time axis in figure 2) is extracted. From the activity, fluorescence probability, Si(li) detectors efficiency, thickness of the activated target and from the beam temporal profile is extracted the total fusion cross section. The present total fusion cross-section and that one measured in [7, 6] is shown in figure 3.

3 Elastic scattering angular distribution and total reaction cross-section.

In well bound nuclei the Optical Potential (OP) $U(E) = V(E)+iW(E)$ used to analize the elastic scattering measure-

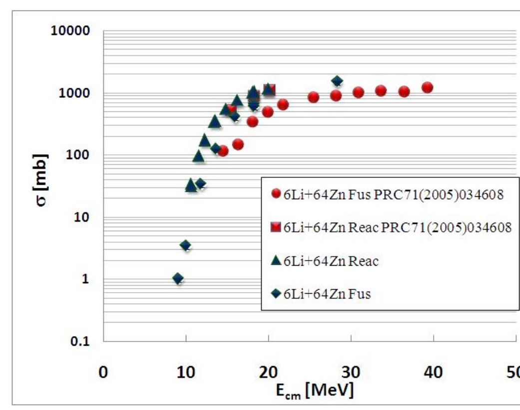

Fig. 3. Present total reaction cross-section (blue triangles) and total fusion cross-section (blue diamonds) are compared with the total reaction cross-section (red squares) and total fusion cross-section (red dots) measured in [7, 6].

ments shows a rapid variation with the energy in the vicinity of the Coulomb barrier. Such a rapid and localized variation is known as the “threshold anomaly” (TA) [15]. The decrease of the absorbitive potential (W(E)) is related to the closure of nonelastic channels at sub-barriers energies. The energy dependence of the real part of OP (to which the term ”anomaly” historically refers) originates from coupling to other channels that give rise to a correction of the real potential. For weakly bound projectiles the break-up channel is expected to be opened also at energies around or below the Coulomb barrier and the usual TA may disappear. Such a phenomenon is known as break-up threshold anomaly (BTA) [15, 5, 8–13]. In this case the strength of the imaginary potential even increases as the incident energy decreases around the barrier. In order to investigate the possible presence of the BTA in the ^{6}Li+^{64}Zn optical potential, a precise elastic scattering angular distributions at several energies around the Coulomb barrier was also performed. It is also usefull in order to extract the total reaction cross-section and compare it with the total fusion cross-section

The measure of the elastic scattering angular distribution at low energy is a difficult task because, in this case, the Coulomb scattering is dominant. Therefore, to see variation with respect to the Coulomb scattering it is necessary to measure with an accuracy of the order of 1% and to go to very backward angles. The experimental set-up is made of an array of five ΔE(10-μm thick)-E(200-μm thick) silicon telescopes placed on a rotating plate that allows to cover a wide angular range. Cross sections absolute values were obtained by normalizing the data with the cross-section measured by two monitor detector placed a small angles, assuming that at small angles the elastic scattering is purely Rutherford scattering.

The total reaction cross-section was obtained fitting the elastic scattering angular distribution with the optical potential. It is shown in figure 3 (blue triangles) togheter with the total reaction cross-section measured in [7]. The two cross-section are in good agreement. The difference between tha total reaction cross-section and the total fusion cross-sections is mainly the break-up contribution. In the present data the break-up contribution is smaller than that one extracted in [7]. It is important to notice that the relative break-up contribution is larger at sub-barrier energies.

3.1 Optical potential analysis.

The angular distributions have been fitted using different optical model potentials [8]: renormalized double folding potential for both real and imaginary part (DF1); renormalized double folding poteturi campanazzantial for the real part and Woods-Saxon potential for the imaginary part (DFWS). In this last case two different density distributions have been used for the double folding potential (DF1WS & DF2WS). The results are displayed in figure 4.

In figure 4-up we see the normalization factors from the fit using the double folding potential for both real and imaginary part (DF1). In figure 4-down we see the other fit with the Woods-Saxon potential for the imaginary part and the two different density distributions for the double folding real potential (DF1WS and DF2WS). Solid symbols, in the right picture, correspond to the DF2WS fit; empty symbols, in the same picture, correspond to the DF1WS fit. Results of independent measurements at a fixed energy, which are plotted in different colours, agree always together. As we observe in both pictures, the optical potential trend is the same independently by the potential used for the fit. As it can be seen from figure , around the Coulomb barrier, indicated by the arrow, there is no presence of usual threshold anomaly.

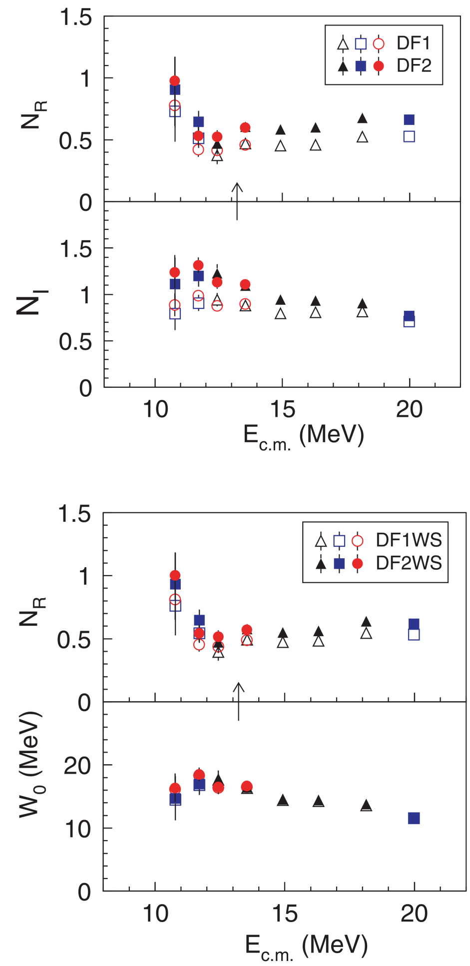

Fig. 4. Trend of the optical model potential obtained by fitting the elastic scattering angular distributions with two different potentials from [8]. Renormalized double folding potential for both real and imaginary part (DF1); renormalized double folding potential for the real part and Woods-Saxon potential for the imaginary part (DF1WS, DF2WS). See the text for details.

4 Conclusions.

The total fusion excitation function for the ^{6}Li+^{64}Zn was measured by using the activation technique. The present fusion excitation function is systematically larger than the one reported in [7]. This result seems to confirm the presence of experimental problems in the ^{6}Li+^{64}Zn fusion data of [7] as suggested by the same authors of [7] in [6]. These problems probably arise from the energy threshold in the direct detection of the evaporation residues, while the activation technique is not affected by this kind of problems. The difference between the total reaction cross-section and the total fusion cross-section, mainly due elastic break-up cross-section is now smaller than in [7]. Moreover, as expected, this comparison shows that the relative contribution of the break-up to the total reaction cross-section become more important when decreasing the beam energy below the barrier. From the analysis of the elastic scattering angular distributions within the optical model, the energy dependence of the optical potential around the Coulomb barrier has been studied showing absence of the usual threshold anomaly.

References

1. L.F. Canto et al., Phys. Rep. C **424**, (2006) 1
2. C.Beck et al., Phys. Rev. C **67**, (2003) 054602
3. Di Pietro A et al., Phys Rev. C **69**, (2004) 044613
4. Di Pietro A et al., Phys Rev. C **69**, (2004) 044613
5. J. M. Figueira, Phys.Rev. C **73**, (2006) 054603
6. P.R.S. Gomez et al., Phys.Rev. C **79**,(2009) 027606
7. P.R.S. Gomez et al., Phys.Rev. C **71**,(2003) 034608
8. M.Zadro et al., Phys. Rev. C **80**, 064610 (2009)
9. N.Keeley et al., Nucl. Phys. A **571**, (1994) 326
10. A. M. M. Maciel et al., Phys. Rev. C **59**, (1999) 2103
11. A. Pakou et al., Phys. Lett. B **556**, (2003) 21
12. A. Pakou et al., Phys. Rev. C **69**, (2004) 054602
13. J. M. Figueira et al., Phys. Rev. C **75**, (2007) 017602
14. F.A. Souza et al., Phys. Rev. C **75**, (2007) 044601
15. G.R. Satchler, Phys. rep. **199** (1991) 147